

Developing a new weir type using the smoothed particle hydrodynamic model

Haris Kalajđisalihović^{*1}, Zoran Milašinović^{1a} and Alen Harapin^{2b}

¹Faculty of Civil Engineering, University of Sarajevo, Patriotske lige 30, Sarajevo, Bosnia and Herzegovina

²Faculty of Civil Engineering, Architecture and Geodesy, University of Split, Matice Hrvatske 15, Split, Croatia

(Received June 28, 2021, Revised August 25, 2021, Accepted October 11, 2021)

Abstract. The aim of this paper is to conduct a hydrodynamic analysis of fluid flow over different weir types using the analytical solution, the physical model taken from another article, and numerical simulations through the Smoothed particle hydrodynamic method (SPH) using the compiled DualSPHysics source code. The paper covers the field of real fluid dynamics that includes a description of different proposed types of weirs in various flow regimes and the optimal solution for the most efficiency structure shape. A detailed presentation of the method, the structure and its characteristics are included. Apart from the single stepped weir, two other weir types are proposed: a Divided type and a Downstream slopped type. All of them are modeled using the SPH method.

Keywords: hydraulic structures; single stepped weir; smoothed particle hydrodynamics; weir

1. Introduction

Weirs within open watercourses are constructed to achieve critical water depth, local equalization of inertial and gravitational forces and the formation of a free water level so that the structure can be used as different type of hydraulic structures with possibility of measuring discharges.

This paper refers to the broad crested weir, the stepped weir, and the developed new type of weir, called the downstream slopped weir. A broad crested weir has large values of ratios L/y_0 and P/y_0 , Fig. 1(a), forms horizontal streamlines so hydrostatic pressure distribution is valid, Chow (1959). Hydraulic structures, in open channel flow, accumulate energy, so significant attention should be paid to erosion prevention, dissipating accumulated energy or protecting the bottom and slopes, Chanson (2001)

Broad crested weirs and exploring the characteristics of that flow have captured the attention of many researchers. The first research on this topic was done by Bazin (1896). He showed the flow capacity of this object. After him, models were developed, and other authors worked on them in the following works (Chow 1959, Woodburn 1932, Hall 1962, Ramamurthy 1988, Gonzalez 2007).

As an improved weir, that has higher energy dissipation efficiency, a single stepped weir is used. After calibrated SPH model for the single stepped weir, simulation for the flows over proposed types of weirs

*Corresponding author, Assistant Professor, E-mail: haris.halajdzi@gmail.com

^aProfessor, E-mail: zoran.milasinovic@gf.unsa.ba

^bProfessor, E-mail: alen.harapin@gradst.hr

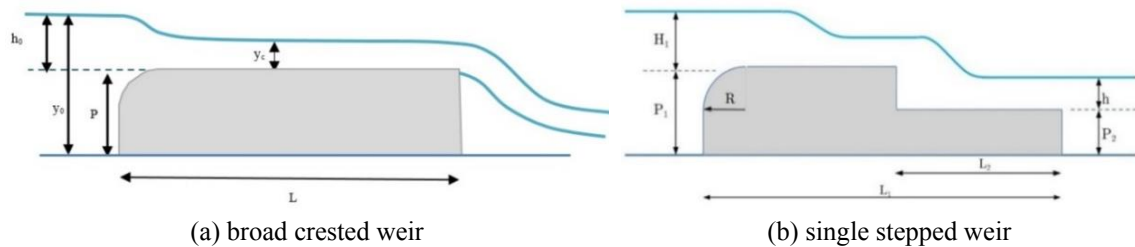


Fig. 1 Schematic representation of the broad crested weir and the single stepped weir

are done.

2. Previous research

The discharge coefficient increases by about 8% if the upstream side of the weir is hydraulically modelled, Woodburn (1932). Mr. Henderson (1966) derived relations to define the discharge coefficients. Ramamurthy *et al.* (1988) investigated the relations for smoothing (R)/height (P) ratio, and gave that in the range $0.094 < R/P < 0.250$, Fig. 1 (left), the increase of the discharge coefficient is obtained. Hussein *et al.* (2009) gave a different form of the broad crested weir than the traditional one that reduces the downstream weir height to dissipate as much energy as possible. In the experiment, they showed that this type of weir dissipates up to 46% more energy than the traditional broad crested weir, and the discharge coefficients become higher. Hamid *et al.* (2010) evaluated the parameters of discharge coefficients and the percentage of the dissipated energy of a single stepped weir. They showed that the ratio of the length of the downstream step in relation to the total length of the weir $L_2/L_1=0.5$ gives a higher energy dissipation compared to other weir models. Recently, the Computational Fluid Dynamics (CFD) was used to find an adequate model for describing flows on these objects. Yazdi *et al.* (2010) in their research performed three-dimensional simulations of Reynolds equations by the Volume of Fluid (VOF) method using the $k-\varepsilon$ open-flow turbulence model. Sarkar and Rhodes in their research work (Sarker and Rhodes 2004) compared the water surfaces levels over a broad crested rectangular weir in laboratory conditions and the numerical analysis. For lower values of discharges, the results fit well. Gonzalez and Chanson (2007) performed numerical analyses of velocity and pressure fields by network-based methods. Hargreaves *et al.* (2007) gave validation for experimental results, published in Hager and Schwalt (1994), through a numerical model for free-surface flow. As a result, they commented on the possibility of applying a numerical model solved by the mesh-based method. Afshar and Hooman (2013) gave results of numerical simulations by the VOF method for broad crested weir conditions with a smoothed edge. The numerical results show a good fit to the experimental results. Hooman (2014) performed a numerical simulation on a triangular broad crested weir using three turbulence models: the Renormalization Group (RNG $k-\varepsilon$), the standard $k-\varepsilon$, and the large eddy simulation (LES) model. The results show the best fit for the RNG $k-\varepsilon$ model. Al-Hashimi *et al.* (2015) used computational mechanics together with a laboratory model to improve the discharge characteristics over a broad crested weir by reducing the possibility of jet separation. They showed that by increasing the upstream slope by 23° the broad crested weir, in terms of flow, has a higher efficiency by 22%.

3. Analytical solution for the broad crested weir

3.1 The water level equation

The differential equation for a steady state, slightly variable flow in an open channel, described by Chow, is used to describe a slightly variable flow (Chow 1959).

$$\frac{dy}{dx} = \frac{S_0 - S_f}{1 - \frac{\alpha Q^2 T}{gA^3}} \quad (1)$$

where: y -depth, x -line coordinate in the direction of flow, S_0 -bottom slope, S_f -slope of the energy line, Q -discharge, T -width of the water face, g -gravitational acceleration, A -cross-section area, α -Coriolis coefficient

For a special case of a channel with a rectangular cross-section $q = \frac{Q}{T}$, $R=y$ and $A=yT$ applies and assuming that $\alpha=1$ the Eq. (1) takes the form

$$\frac{dy}{dx} = \frac{S_0 - S_f}{1 - \frac{q^2}{gy^3}} \quad (2)$$

with critical depth

$$y_c = \sqrt[3]{\frac{q^2}{g}} \quad (3)$$

and $S_0=0$, Eq. (2) becomes

$$\frac{dy}{dx} = \frac{-S_f}{1 - \left(\frac{y_c}{y}\right)^3} \quad (4)$$

Introducing the Maning's equation

$$S_f = \frac{q^2 n^2}{y^3} \quad (5)$$

Eq. (4) becomes

$$\frac{dy}{dx} = \frac{-\frac{q^2 n^2}{y^3}}{1 - \left(\frac{y_c}{y}\right)^3} \quad (6)$$

with further substitutions: $k = -q^2 n^2$; $\lambda = \frac{y}{y_c}$; $\frac{d\lambda}{dy} = \frac{1}{y_c}$; $k_1 = \frac{k}{y_c^{\frac{13}{3}}}$

and by integrating

$$x = \frac{1}{k_1} \left(\frac{3}{13} \lambda^{\frac{13}{3}} - \frac{3}{4} \lambda^{\frac{4}{3}} + c \right) \quad (7)$$

The integration constant is determined from the boundary conditions, i.e., $y=y_c$.

For the broad crested weir and the similar single stepped weir $L_2/L_1=0,5$; the discharge is $Q=19,85$ l/s; $n=0,011$; and y_c implies $x=-17,25$ cm, the value of the constant is 0.735. Eq. (7) for this particular solution thus becomes

$$x = \frac{1}{k_1} \left(\frac{3}{13} \lambda^{\frac{13}{3}} - \frac{3}{4} \lambda^{\frac{4}{3}} + 0.735 \right) \quad (8)$$

3.2 The discharge coefficient

There is a functional dependence of the flow coefficient on the main flow parameters, as in Fig. 1 right

$$f_1(q, H, P_1, L, R, P_2, L_2, g, \nu) \quad (9)$$

where:

q -discharge over weir, H -upstream water depth (above the weir height), P_1 -upstream height of the weir, L -weir length, R -radius of curvature on the upstream side, P_2 -downstream weir height, L_2 -length of the downstream step, g -gravitational acceleration, ν -kinematic viscosity coefficient

From the dimensional analysis

$$C_d = \frac{q}{\frac{2}{3} H \sqrt{\frac{2}{3} g H}} = f_2 \left(\frac{H}{P_1}, \frac{L}{P_1}, \frac{R}{P_1}, \frac{P_2}{P_1}, \frac{L_2}{P_1}, Re \right) \quad (10)$$

where Re is the Reynolds number, which in this case has a very large value, so its influence on the flow coefficient is very small and can be neglected.

If the individual parameters are taken as fixed values then the coefficient will also not depend on them.

In the Ramamurthy *et al.* (1988) study, the force resulting from the shear stress on the contour is introduced into the mass conservation.

$$F_1 + M_1 = F_p + F_3 + M_3 + F\tau_0 \quad (11)$$

$$F\tau_0 = \tau_0 \cdot B \cdot L = \mu \frac{dv}{dy} BL \quad (12)$$

For the inlet and outlet cross-section the control volume of the considered flow over the broad crested weir is

$$F\tau_0 = \frac{v_1 - v_2}{H - h} \cdot \mu \cdot B \cdot L \quad (13)$$

Substituting

$$Q = v_1 \cdot B \cdot H = v_2 \cdot B \cdot h \quad (14)$$

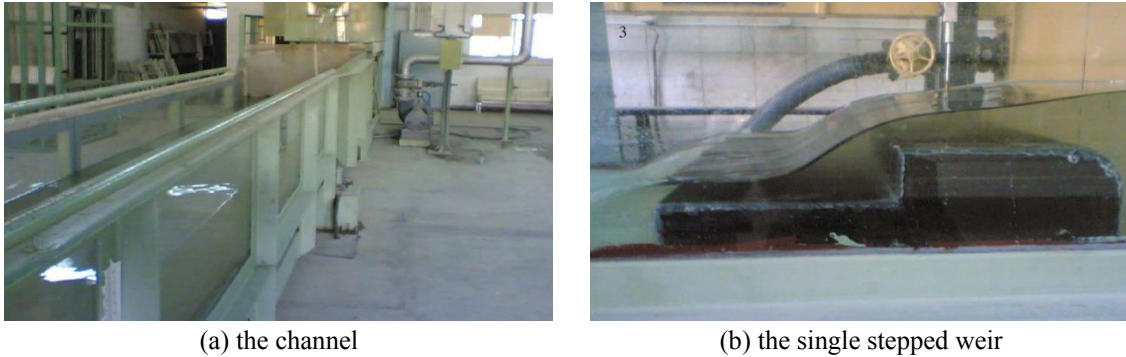


Fig. 2 Photo of the experimental channel equipped with a single stepped weir

it becomes

$$F\tau_0 = -\frac{Q\mu L}{Hh} \tag{15}$$

where:

$F\tau_0$ -shear force along the contour, τ_0 -shear contour stress, Q -discharge, v_1 -velocity at the inlet section, v_2 -speed at the outlet cross section, downstream, B -channel width, L -weir length, μ -dynamic viscosity coefficient, h -downstream water depth

Further, the same author (Ramamurthy 1988) gives the complete equation

$$\frac{\gamma}{2}(H + P_1)^2 B + \frac{\gamma}{g} \left(\frac{Q}{(H + P_1)^2 B} \right) = k_p \frac{\gamma}{2} [P_1(2H + P_1)B] + \frac{\gamma}{2} h^2 B + \frac{\gamma Q^2}{ghB} - \frac{Q\mu L}{Hh} \tag{16}$$

and gives as a recommendation $k_p=0,98$.

The equation for flow over the broad crested weir is given as

$$Q = C_d \frac{2}{3} HB \sqrt{\frac{2}{3} gH} \tag{17}$$

and further

$$(H + P_1)^2 - h^2 - k_p [2(2H + P_1)B] = \frac{16}{27} H^3 C_d^2 \left[\frac{1}{h} - \frac{1}{H + P_1} \right] - \frac{4\mu L}{3\gamma h} \sqrt{\frac{2}{3} gHC_d} \tag{18}$$

The final form is

$$A_1 C_d^2 - A_2 C_d - A_3 = 0 \tag{19}$$

where:

$$A_1 = \frac{16}{27} H^3 \left[\frac{1}{h} - \frac{1}{H + P_1} \right]; \quad A_2 = \frac{4\mu L}{3\gamma h} \sqrt{\frac{2}{3} gH}; \quad A_3 = (H + P_1)^2 - h^2 - k_p [P_1(2H + P_1)]$$

and the solution

$$C_{d_{1,2}} = \frac{A_2}{2A_1} \mp \left[\left(\frac{A_2}{2A_1} \right)^2 + \frac{A_3}{A_1} \right]^{1/2} \tag{20}$$

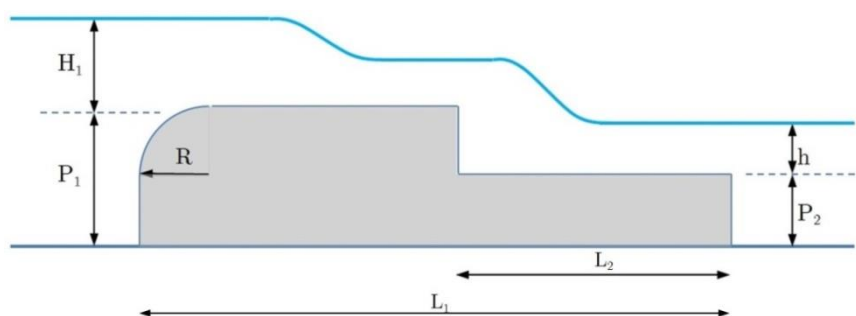


Fig. 3 Schematic representation of a single stepped weir

Table 1 Observed data from the experiment (Hamid 2010) and the calculated discharge coefficient values

No	L_i (cm)		L_2/L_1	H (m)	q (cm ² /s)	C_d
1-7	L_1	48	0.5	0.12-0.22	139-631	0.954-0.988
	L_2	24				

4. Physical modeling of a single stepped weir

Hamid (2010) performed the experiment on a channel with a horizontal bottom, with dimensions: 0.5 m wide, 10 m long, 0.45 m high. The dimensions of the weir were variable lengths L_1 and L_2 shown in Fig. 3 and fixed values of parameters $P_1=12$ cm, $P_2=6$ cm, $R=6$ cm. The results of the experiments taken from the work are shown in Table 1.

Other observed data such as the discharge coefficients and the levels of energy dissipation of the physical model, described in paper (Hamid 2010), are used further in this paper.

Energy dissipation

The purpose of the single stepped weir is to increase the flow coefficient C_d and the energy dissipation ΔE (%).

According to Hamid *et al.* (2010), the percentage of the dissipated energy related to the dimensional analysis is

$$E(\%) = 6.56 \left(\frac{h}{P_1} \right)^{-0.27} \left(\frac{P_2}{P_1} \right)^{-1.4} \quad (21)$$

5. The Smoothed Particle Hydrodynamics (SPH) model

5.1 SPH formulation

This method is Lagrange's, mesh-less, particle method with special characteristics. It has some special advantages compared to traditional methods whose domain is discretized by the mesh. Its biggest advantage is adaptability, so in each subsequent time step, the particles are adapted to change the domain.

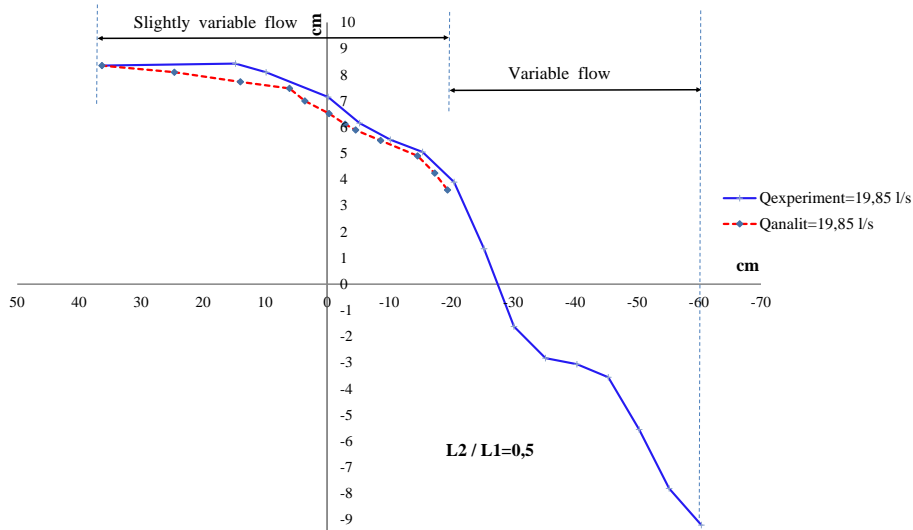


Fig. 4 The results of water levels for the chosen discharge of 19.85 l/s-experimental for the single stepped weir (Hamid 2010) and analytical for the broad crested weir

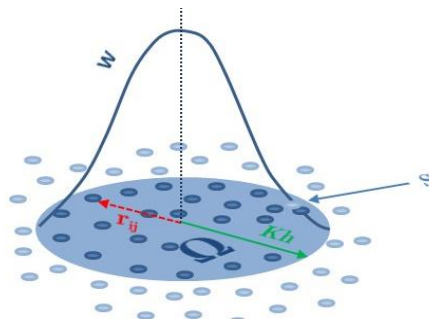


Fig. 5 Kernel function approximation

The entire fluid flow in fluid mechanics is described by partial differential equations. The solution will be given as the approximation of functions and its derivatives at each point.

The formulation of the SPH method is given into two steps. The first step is an integral representation of the so-called Kernel approximation of the field function, while the second step is the approximation of the particles.

5.1.1 Kernel approximation

The concept of the integral representation of a function used in the SPH method begins with the relation

$$f(x) = \int_{\omega} f(x') \delta(x-x') dx' \tag{22}$$

f is a function of the position of the vector x .

The Dirac delta function is given as: $\delta(x-x') = \begin{cases} 0, & x = x' \\ 1, & x \neq x' \end{cases}$

Substitute the Dirac delta with the Kernel function W

$$\langle f(x) \rangle = \int_{\omega} f(x)W(x-x',h)dx' \quad (23)$$

If in the above Eq. (23) for the Kernel function $f(x)$ is replaced with $\nabla f(x)$ it becomes

$$\langle \nabla f(x) \rangle = \int_{\omega} [\nabla f(x')]W(x-x',h)dx' \quad (24)$$

Introducing the chain rule and applying it to Eq. (24) it becomes

$$\langle \nabla f(x) \rangle = \int_S f(x')W(x-x',h)\vec{n}dS - \int_{\omega} f(x')\nabla W(x-x',h) \quad (25)$$

\vec{n} -unit vector, perpendicular to the surface S .

When the Kernel function satisfies the rule $W(x-x',h)=0$ for all $(x-x')>Kh$, the first member on right-hand side of Eq. (25) is equal to zero, and:

$$\langle \nabla f(x) \rangle = - \int_{\omega} f(x')\nabla W(x-x',h) \quad (26)$$

In Eq. (26) the derivative of the function is written as the product of the value of the function and the derivative of the Kernel function. This interpretation is most similar to methods with a weak form in which the needs of consistency are reduced to the assumed field of the function and thus it makes a stable solution of the Partial differential equations.

5.1.2 Approximation of the particles

The entire domain is described by a set, finite number of particles. Particles have individual mass and take their places in space.

$$m_j = \Delta V_j \rho_j \quad (27)$$

ρ_j -unit mass of particle hence it is

$$f(x) = \sum_{j=1}^N \frac{m_j}{\rho_j} f(x_j)W(x-x_j,h) \quad (28)$$

and for particle approximation it is

$$\langle f(x_i) \rangle = \sum_{j=1}^N \frac{m_j}{\rho_j} f(x_j)W_{ij} \quad (29)$$

where $W_{ij}=W(x_i-x_j,h)$ and according to Eq. (26)

$$\langle \nabla f(x_i) \rangle = - \sum_{j=1}^N \frac{m_j}{\rho_j} \nabla W_{ij} \quad (30)$$

5.1.3 Kernel function

The kernel function is the basis of the SPH method. It defines the accuracy and the efficiency of the calculation. The Kernel function has to satisfy a few conditions, it has to:

- be normalized

$$\int_{\omega} W(x-x', h) dx' = 1 \tag{31}$$

- have the same values as the Dirac delta at the end of the domain

$$\lim_{h \rightarrow 0} W(x-x', h) = \delta(x-x') \tag{32}$$

- be equal to zero out of the domain

$$W(x-x', h) = 0 \tag{33}$$

- be monotonically decreasing towards the edge of the domain
- be smoothed
- be symmetric

In this paper, the Wendland (1995), Panizzo *et al.* (2007) function is used as

$$W(r, h) = \alpha_D \left(1 - \frac{q}{2}\right)^4 (2q+1) \tag{34}$$

In the $0 \leq q \leq 2$ domain, for the coefficient $\alpha_D = \frac{7}{8\pi h^3}$ in 3D space

5.1.4 Boundary conditions

The dynamic boundary condition was used within this paper due to faster calculations. It was first used by Darymple and Knio (2001), and was also explained in detail by Crespo *et al.* (2007). This method is computationally much simpler than the other ones, because both the boundary and the fluid consist of the same particles, so the same loop within the code can be used for both. It is necessary to make a border of the so-called boundary particles, usually two or three rows of particles, so that the condition of normalization of the Kernel function would not be questionable. The boundary particles take on all the values of the functions like the fluid particles, except that they have no displacements and are fixed in a given position.

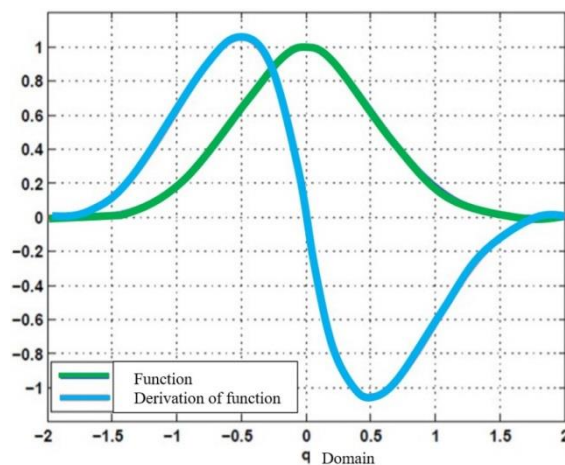


Fig. 6 Normalized Wendland Kernel function and its first derivation

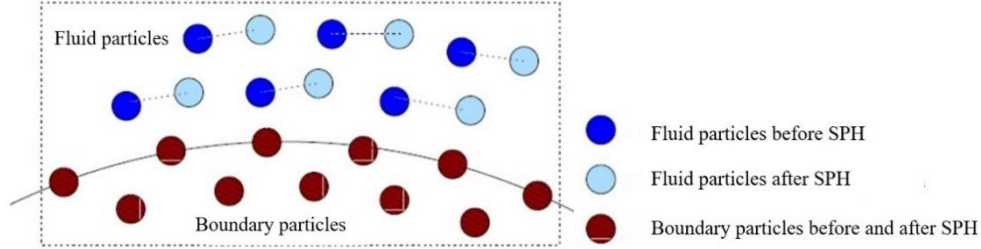


Fig. 7 Dynamic boundary condition

5.2 The Navier-Stokes equations in the SPH

5.2.1 Mass conservation

$$\rho_i = \sum_j m_j W_{ij} \quad (35)$$

5.2.2 Momentum conservation

$$\frac{dv_i}{dt} = -\sum_j m_j \left(\frac{P_i}{\rho_i^2} + \frac{P_j}{\rho_j^2} \right) \nabla_i W_{ij} + g + \sum_j m_j \left(\frac{4\nu_0 r_{ij} \nabla_i W_{ij}}{(\rho_i + \rho_j) |r_{ij}|^2} \right) v_{ij} \quad (36)$$

Eq. (36) describes the laminar viscosity. Favre averaging can also expand Eqs. (35) to (36) by an additional unit force per unit volume, produced by the turbulent viscosity (Sub particle scale-SPS) when it takes shape, as reported by Darymple and Rogers (2006).

$$\frac{dv_i}{dt} = -\sum_j m_j \left(\frac{P_i}{\rho_i^2} + \frac{P_j}{\rho_j^2} - \frac{\tau_i^t}{\rho_i^2} + \frac{\tau_j^t}{\rho_j^2} \right) \nabla_i W_{ij} + g + \sum_j m_j \left(\frac{4\nu_0 r_{ij} \nabla_i W_{ij}}{(\rho_i + \rho_j) |r_{ij}|^2} \right) v_{ij} \quad (37)$$

$$\frac{\tau_{ij}^t}{\rho} = 2\nu_t S_{ij} - \frac{2}{3} C_I \Delta^2 \delta_{ij} |S_{ij}|^2 \quad (38)$$

τ_{ij}^t -SPS turbulent stress, ν_t -coefficient of turbulent viscosity $\nu_t = [\min(C_S, \Delta l)]^2$, S_{ij} -SPS tensor element, $C_I = 0,0066$, C_S -Smagorinsky constant (0,12).

5.2.3 Equation of state

Equation of state is taken into the calculation in order to create artificial compressibility and fictitiously reduce the propagation speed of the elastic wave, which could significantly increase the integration step in the calculation, while the Courant-Friedrich-Levy (CFL) criterion on the stability of a numerical solution is satisfied.

$$P = B \left[\left(\frac{\rho}{\rho_0} \right)^\gamma - 1 \right] \quad (39)$$

$$B = \frac{c_0^2 \rho_0}{\gamma}; c_0\text{-speed of the elastic wave; } 1 \leq \gamma \leq 7$$

5.2.4 Energy conservation

$$\frac{de}{dt} = \frac{1}{2} \sum_j m_j \left(\frac{P_i}{\rho_i^2} + \frac{P_j}{\rho_j^2} + \Pi_{ij} \right) v_{ij} \nabla_i W_{ij} \quad (40)$$

5.2.5 Mass recalculation

Molteni and Colagrossi (2009) apply the deltaSPH formulation to recalculate unit mass and reduce the oscillation of the specific mass field values. It uses the diffusion condition in the mass conservation equation

$$\frac{d\rho_i}{dt} = D_i^{n+1} \sum_j m_j v_{ij} \nabla_i W_{ij} + 2\delta_\Phi h c_0 \sum_j (\rho_j - \rho_i) \frac{r_{ij} \nabla_i W_{ij}}{r_{ij}^2} \frac{m_j}{\rho_j} \quad (41)$$

For time integration, the Predictor-Corrector (Symplectic) scheme is used.

6. The SPH Model set up in the DualSPHysics code

Three models are done in this article. The first one describes streaming over a single stepped weir and is compared to the physical model's water levels, level of energy dissipation and discharge coefficients. The other two models are proposed in this article as new types of weirs and compared to the first one and also to the data observed on physical model. Channel geometry, described in Fig. 8, is used for all three types of weirs.

6.1 The SPH model of the single stepped weir

Model settings parameters:

Dimensions of the weir given in Fig. 8

Channel length 6m

Channel width 0.5 m

Channel depth 0.5 m

$P_1=12$ cm, $P_2=6$ cm, $L_1=48$ cm, $L_2=24$ cm, $R=6$ cm

Fluid particle size: 0.015 m

Dynamic fluid viscosity: 10^{-6} m²/s

Integration scheme: Symplectic

Accuracy: Single

Multiplication factor for the friction force with a solid structure in relation to the viscosity of the fluid: 10000 (the coefficient of friction in contact with the type of structure is 10000x higher than in the fluid-fluid relationship)

Specific mass correction: each time step deltaSPH

Flow control was performed by a tabular gate and water level in the upstream reservoir

Level in the upstream tank: 0.5 m

Clearance under the gate plate: 0.09 m to achieve $Q=19.85$ l/s. Other clearances are used to

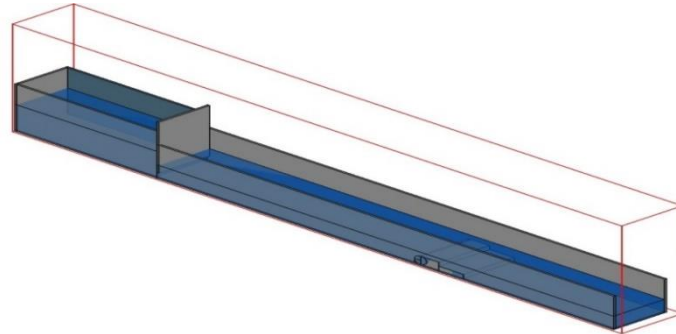


Fig. 8 Modeled channel flow with a single stepped weir

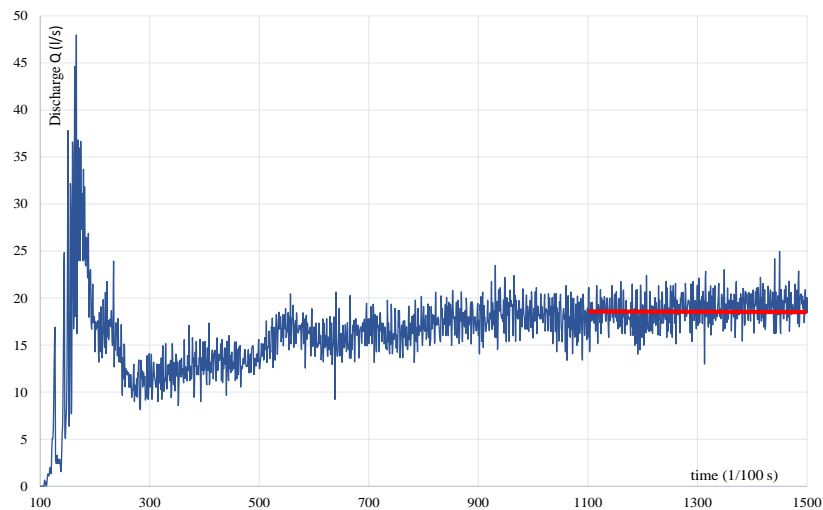


Fig. 9 Discharges in the channel over time. The average value of 19.85 l/s is reached after 11 s of simulation

achieve other values, $Q=15.50$ l/s and $Q=9.55$ l/s, $Q=26.50$ l/s and $Q=31.55$ l/s

Downstream boundary condition: horizontal bottom and recirculating water into the upstream tank

Number of particles: 466000

Simulation time: 15s

Output frequency .vtk files: 100 Hz

Computer simulation time, GPU nVidia GeForce 1050Ti: 12h 50min

Postprocessor: ParaVIEW 5.6.0

6.2 The SPH model for the other two proposed weir types

After modelling the proposed types of weirs, the calculation of energy dissipation is as

$$\Delta E = E_1 - E_2 \quad (42)$$

$$\Delta E (\%) = \frac{E_1 - E_2}{E_1} \cdot 100 \quad (43)$$

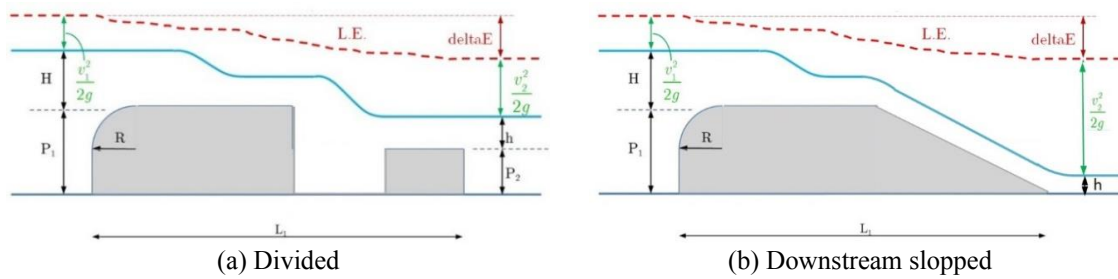


Fig. 10 Drawings of the proposed types of weirs

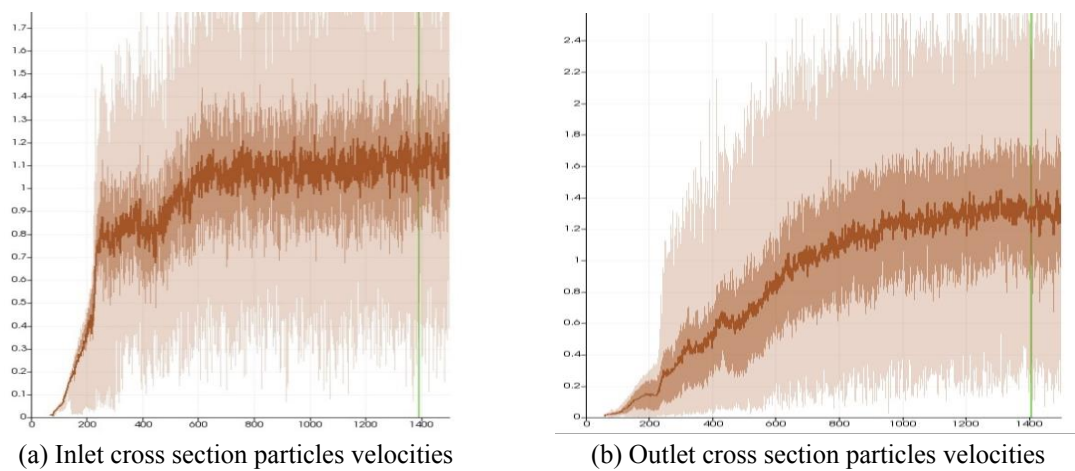


Fig. 11 Output modeled values of time dependent velocities

The kinetic part of energy calculation is based on the averaged cross section velocity.

6.3 Results of SPH modeling

This paper shows the Smoothed Particle Hydrodynamic model results for all three considered weir types. The single stepped weir model is based on the observed laboratory results taken from (Hamid 2010) and is the basis for modeling the other two proposed types. The proposed types aim to increase energy dissipation and reduce the volume of physical laboratory research.

The results of this paper present comparative values of the three considered weirs together with the results taken from laboratory research, (Hamid 2010). The results are given through water levels of individual objects, with the analytical solution in the domain of its existence, for discharge $Q=19.85$ l/s (Fig. 14); through energy dissipations for the three considered discharge values: $Q=19.85$ l/s, $Q=26.50$ l/s and $Q=31.55$ l/s (Fig. 15); and for the discharge coefficients also for the three considered discharge values: $Q=19.85$ l/s, $Q=15.50$ l/s and $Q=9.55$ l/s (Fig. 12).

7. Conclusions

The used SPH model simulates the flow over a single stepped weir. Set up dimensions are: $L_2=48$

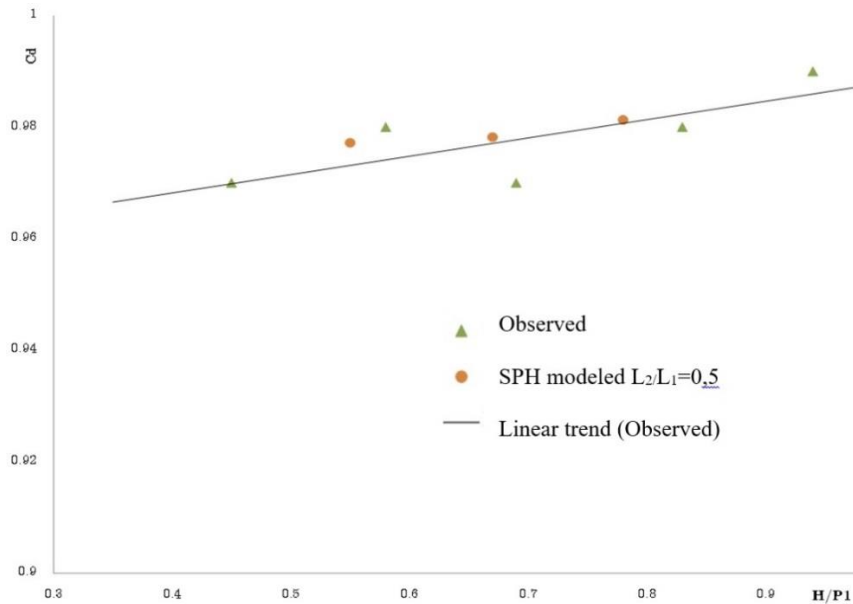


Fig. 12 Discharge coefficients for the observed (Hamid 2010) and the SPH modeled data (single stepped weir)

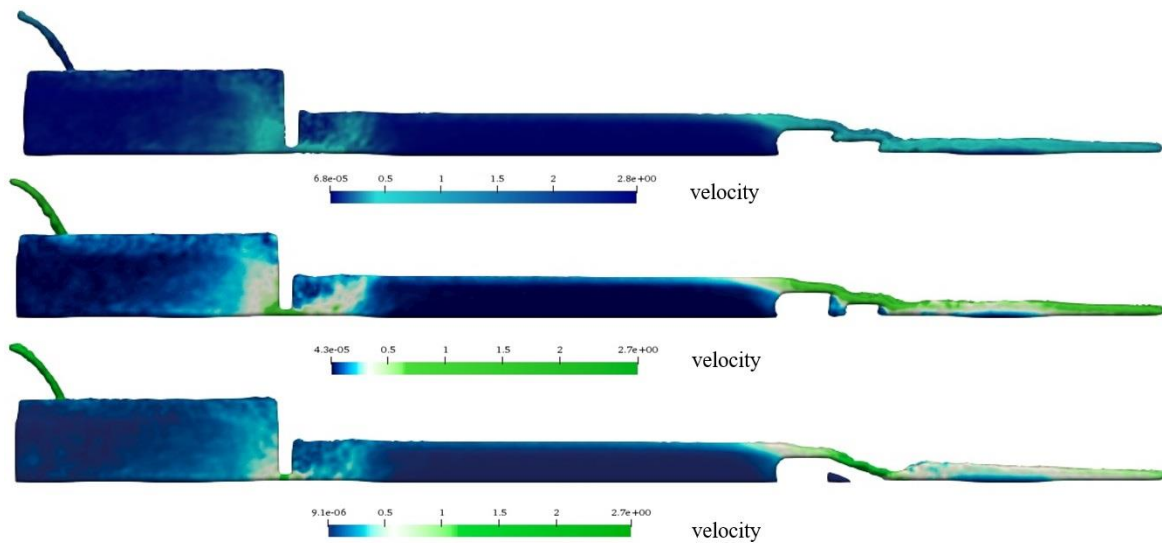


Fig. 13 Modeled water levels and velocities of the three selected weir types at $t=13s$. $Q=19.851/s$

cm, $L_1=24$ cm, $R=6$ cm, $P_1=12$ cm and $P_2=6$ cm with the width of 0.5 m. The results of the SPH single stepped weir model in terms of water levels, energy dissipation, and flow coefficients, fits the observed data well. The SPH model was used to develop a new type of weir, called the Downstream sloped weir, which has higher rate of energy dissipation than the single stepped weir for considered discharges.

This paper gave a detailed overview of previous works, as well as dimensional, visual and

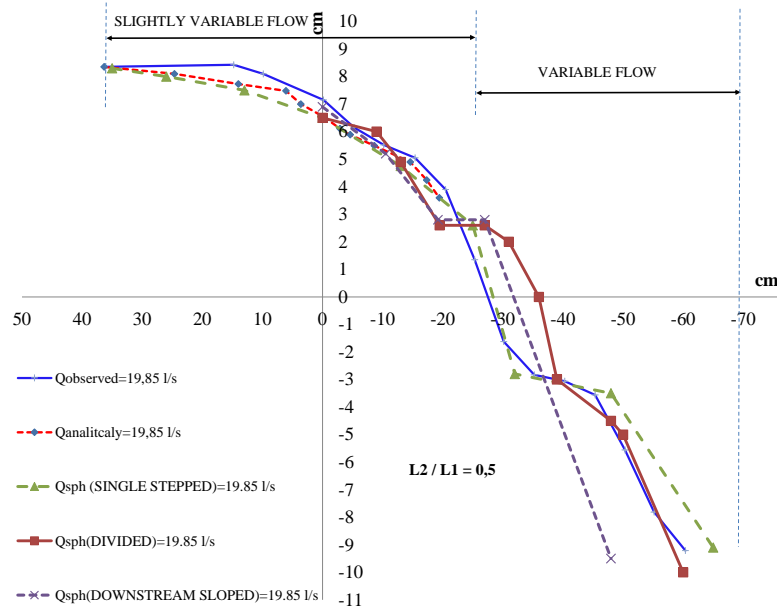


Fig. 14 Comparison of water levels over weirs: analytical, observed (Hamid H. 2010) and modelled

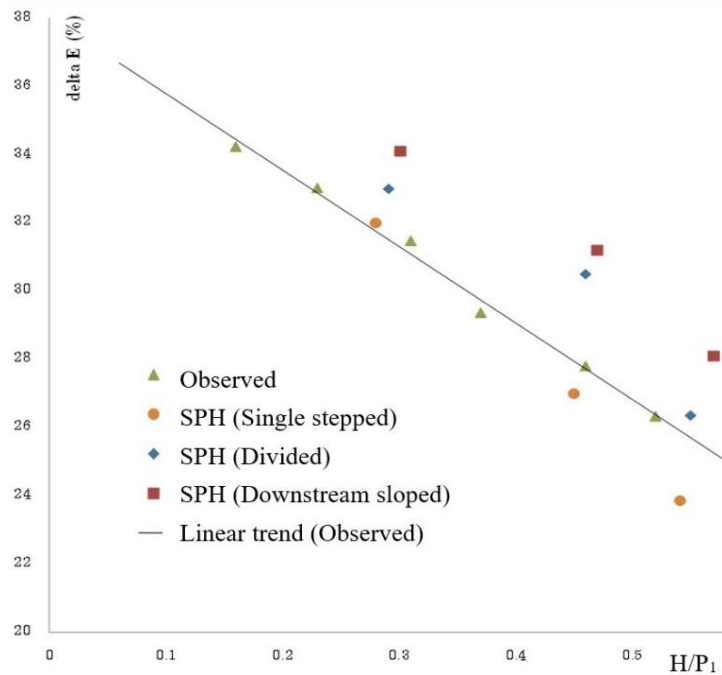


Fig. 15 Relative energy dissipation for physical and SPH numerical models of the three weir types

analytical descriptions of the flow over the weirs.

This paper proposes the Downstream slopped weir, but in further work additional physical measurements will be conducted.

Table 2 Relative energy dissipations according to the type of structure and the discharge

Weir type	E(%) SPH			E(%) Observed		
	Q=9.55 l/s	Q=15.5 l/s	Q=19.85 l/s	Q=9.55 l/s	Q=15.5 l/s	Q=19.85 l/s
Single stepped	32.1	28	23.86	31.7	27.81	26.34
Divided	33.07	30.9	26.35	-	-	-
Downstream slopped	34.1	31.2	28.1	-	-	-

References

- Afshar, H. and Hoseini, S.H. (2013), "Experimental and 3-D numerical simulation of flow over a rectangular broad-crested weir", *Int. J. Eng. Adv. Technol.*, **2**(6), 214-219.
- Al-Hashimi, A.S., Sadeq, A. and Huda, M. (2015), "Determination of discharge coefficient of rectangular broad-crested weir by CFD", *The 2nd International Conference of Buildings, Construction and Environmental Engineering (BCEE2-2015)*, Beirut.
- Bazin (1896), *Open Channel Hydraulics*, McGraw-Hill, USA.
- Chanson, H. (2001), "Hydraulic design of stepped spillways and downstream energy dissipators", *Dam Eng.*, **11**(4), 205-242.
- Chow, V.T. (1959), *Open Channel Hydraulics*, McGraw-Hill, New York.
- Crespo, A.J.C., Gomez-Gesteira, M. and Dalrymple, R.A. (2007), "Boundary conditions generated by dynamic particles in SPH methods", *Comput. Mater. Continua*, **5**(3), 173-184.
- Dalrymple, R.A. and Knio, O. (2001), "SPH modelling of water waves", *The 4th Conference on Coastal Dynamics*, 779-787. [https://doi.org/10.1061/40566\(260\)80](https://doi.org/10.1061/40566(260)80).
- Dalrymple, R.A. and Rogers, B. (2006), "Numerical modeling of water waves with the SPH method", *Coast. Eng.*, **53**, 141-147. <https://doi.org/10.1016/j.coastaleng.2005.10.004>.
- Gonzalez, C.A. and Chanson, H. (2007), "Experimental measurements of velocity and pressure distribution on a large broad-crested weir", *Flow Measure. Instrum.*, **18**, 107-113. <https://doi.org/10.1016/j.flowmeasinst.2007.05.005>.
- Hager, W.H. and Schwalt, M. (1994), "Broad-crested weir", *J. Irrigat. Drain. Eng.*, **120**(1), 13-26. [https://doi.org/10.1061/\(ASCE\)0733-9437\(1994\)120:1\(13\)](https://doi.org/10.1061/(ASCE)0733-9437(1994)120:1(13)).
- Hall, G.W. (1962), "Discharge characteristics of broad-crested weirs using boundary layer theory", *Proceedings of the Institution of Civil Engineers*, London.
- Hamid, H., Inam, A.K. and Saleh, J.S. (2010), "Improving the hydraulic performance of single step broad-crested weirs", *J. Civil Eng.*, **7**(1), 1-12.
- Hargreaves, D.M., Morvan, H.P. and Wright, N.G. (2007), "Validation of the volume of fluid method for free surface calculation: The broad-crested weir", *Eng. Appl. Comput. Fluid Mech.*, **1**(2), 136-146. <https://doi.org/10.1080/19942060.2007.11015188>.
- Henderson F.M. (1966), *Open Channel Flow*, MacMillan, New York.
- Hooman, S. (2014), "3D simulation broad of flow over a triangular broad-crested weir", *J. River Eng.*, **2**(2), 1-7.
- Hussein, H.H., Juma, A. and Shareef, S. (2009), "Flow characteristics and energy dissipation over stepped round-nosed broad-crested weirs", *J. Al-Rafidain Eng.*, **17**, 95-107.
- Molteni, D. and Colagrossi, A. (2009), "A simple procedure to improve the pressure evaluation in hydrodynamic context using the SPH", *Comput. Phys. Commun.*, **180**(6), 861-872. <https://doi.org/10.1016/j.cpc.2008.12.004>.
- Panizzo, A., Capone, T. and Dalrymple, R.A. (2007), "Accuracy of kernel derivatives and numerical schemes in SPH", *Journal of Computational Physics*.
- Ramamurthy, A.S., Tim, U.S. and Rao, M.J. (1988), "Characteristics of square-edged and round-nosed broad-crested weirs", *J. Irrig. Drain. Eng.*, **114**(1), 61-73. [https://doi.org/10.1061/\(ASCE\)0733-](https://doi.org/10.1061/(ASCE)0733-)

- 9437(1988)114:1(61).
- Sarker, M.A. and Rhodes, D.G. (2004), "CFD and physical modelling of free surface over broad-crested weir", Cranfield University, Cranfield.
- Wendland, H. (1995), *Computational Aspects of Radial Basisfunction Approximation*, Elsevier.
- Woodburn, J.G. (1932), "Tests of broad-crested weirs", *Tran. Am. Soc. Civil Eng.*, **96**(1), 387-416. <https://doi.org/10.1061/TACEAT.0004394>.
- Yazdi, J., Sarkardeh, H., Azamathulla, H.M. and Ghani, A.A. (2010), "3D simulation of flow around a single spur dike with free surface flow", *Int. J. River Basin Manage.*, **8**, 55-62. <https://doi.org/10.1080/15715121003715107>.